Projet SAFIRS

Activité Triplets NbTi

Pré-étude mécanique du quadripôle destiné aux futurs Triplets NbTi

1. Introduction

This note presents the first Finite Element Model (FEM) results of the quadrupole straight section for the Triplets NbTi. Numerical computation was realized with the COFAST3D approach, a modular developed from the CASTEM software package.

The magnetic field level is comparable to that of the LHC main quadrupole magnets, but the Lorentz forces are twice higher due to a larger diameter of the bore aperture (120 mm). One aim of this analysis is to verify if the future NbTi coils can be assembled like the LHC main quadrupole collaring process by means of collars individually stacked in alternating layers against the coils. In this case, the iron yoke has not to give a radial support to the collared coil.

Two different mechanical models are studied. The three loading steps which are collaring, cool down and excitation at full current are simulated and stress and displacement appearing in coils and collars are estimated at all phases.

2. Main characteristic of the future NbTi coils

Inner and outer coil layers will be made from the same cables than those used for the LHC main dipoles. The magnetic design is given by CERN (Files 120mm_V24.data and 120mm_V24.iron given by ROXIE [1]). At nominal current of 12720 A and 1.8 K, the field gradient will be of 119 T/m. Due to a larger diameter of the bore aperture, the Lorentz forces will be twice higher than for the LHC main quadrupole. A representation of the conductor blocs' position and of the Lorentz forces distribution at nominal current is given in Fig.1.

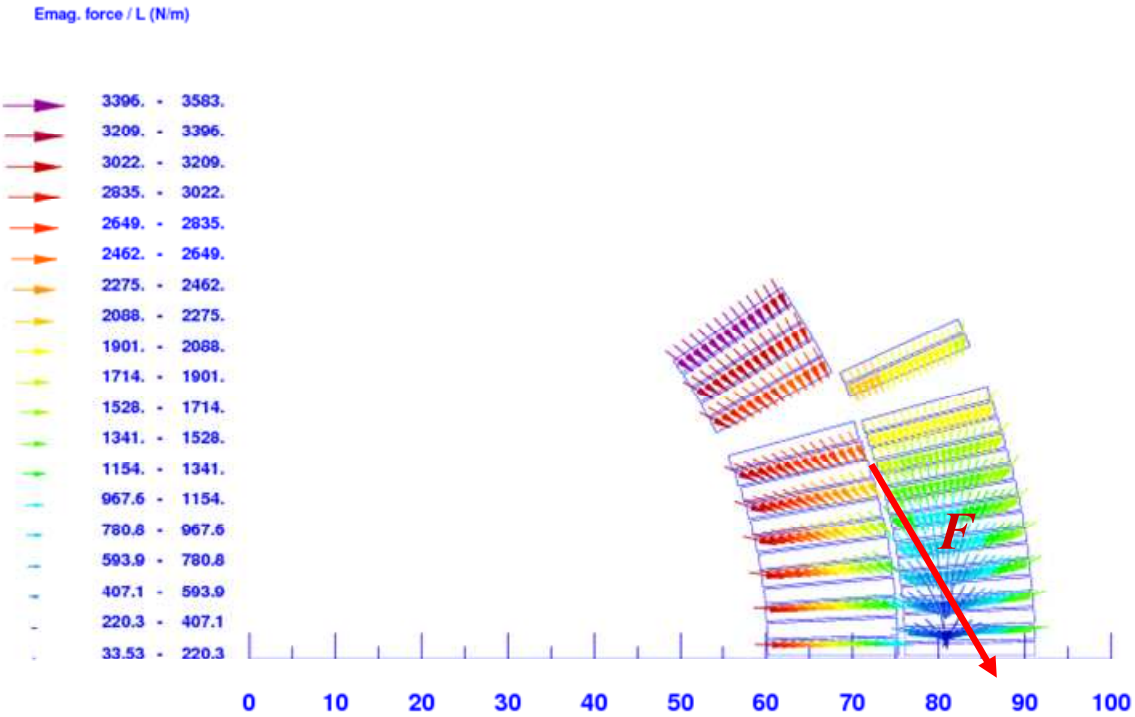

Fig.1: Position of conductor blocs and Lorentz force distribution in one octant coil (ROXIE).
Total per octant: F_x = 937 kN/m, F_y = -1.35 MN/m. F = 1.65 MN/m.

Globally, Lorentz forces tend to move coils away from the polar plan and to squeeze them in the median plan. An azimuthal pre-stress in coils is needed to assure the contact between coils and collars on polar plans during excitation.

3. Material properties

Tab.1 gives material thermo-mechanical properties used for the analytical approach and for computation. Values in red are estimated and need to be experimentally verified:

- it is assumed that the coils Young's Modulus at 2 K is 1.5 times higher than at 300 K. This phenomenon was observed on stacks of conductors both for the LHC main dipoles [2] and for the LHC main quadrupole [3] [4],
- the integrated thermal shrinkage of coil between 300 K and 2 K is estimated to be of 6.5 to 7.5 mm/m.

Materials *Componants*	Temp. (K)	Elastic Modulus (GPa)	Yield Strenght (MPa)	Ultimate Strength (MPa)	Integrated Thermal Expansion (mm/m)
yus 130 S Nippon Steel	300	190	445	795	
Collars	2	210	1023	1595	-2.4 to -2.6
316L Stainless Steel	300	205	275	596	
Keys	2	210	666	1570	-2.9
Copper	300	136			
Angular wedges	2	136			-3.3
Kapton Foils	300	2.5			
Ground & inter-pole insulations	2	4			-6.0
insulated NbTi conductors blocs	300	5.5/4.5			
Coil inner/outer layers	2	8.25/6.75			-6.5 to -7.5

Tab.1: Material properties

For both analytical approximation and calculation, the higher loss of pre-stress during cool-down is taken into account by considering a maximum thermal shrinkage differential between coils and collars. Therefore we used the integrated thermal shrinkage of 7.5 mm/m and of 2.4 mm/m for conductor blocs and for collars, respectively.

4. Analytical approximation of the pre-stress

To compensate the effects of thermal shrinkage differential between coils and collars and to reduce the coil displacement during excitation (due to Lorentz forces), an azimuthal pre-stress should be imposed in coils during the collaring process. A first analytical approximation of the pre-stress σ_{coil} can be given by [4]:

$$\sigma_{coil} \approx -E_{coil}\left(\int_{4K}^{300K} \alpha_{collar}\,dT - \int_{4K}^{300K} \alpha_{coil}\,dT\right) - \frac{2}{3}\frac{F_\theta}{w_{coil}} \qquad (1)$$

where E_{coil} is the mean coil Young's modulus in the azimuthal direction between room and operating temperature. α_{collar} and α_{coil} are the integrated thermal shrinkage of collars and of coils, respectively. F_θ is the azimuthal component of Lorentz forces (per coil unit length) and w_{coil} is the cable radial width. A security margin of 10 MPa will be considered for the pre-stress.

For the quadrupole model, the azimuthal component of magnetic forces is of 853 kN/m for the coil inner layer and of 711 kN/m for the coil outer layer. Finally, studies have shown that a phenomenon of stress relaxation occurs at room temperature after the collaring process [5] [6]. This relaxation is assumed to be of 20 % of the initial stress and is taken into account in the estimation of the pre-stress:

$$\sigma_{in} \approx \left(-6.87\ \text{GPa} \times (7.5\ \text{‰} - 2.4\ \text{‰}) - \frac{2}{3} \times \frac{853\ \text{kN/m}}{15.4\ \text{mm}} - 10\ \text{MPa} \right) \times 1.2 = -98\ \text{MPa}$$
$$\sigma_{out} \approx \left(-5.62\ \text{GPa} \times (7.5\ \text{‰} - 2.4\ \text{‰}) - \frac{2}{3} \times \frac{711\ \text{kN/m}}{15.4\ \text{mm}} - 10\ \text{MPa} \right) \times 1.2 = -83\ \text{MPa} \quad (2)$$

The relaxation has to be experimentally verified, but if it is not considered, the pre-stress should be approximately of 75 MPa (same level than for the LHC main dipoles and quadrupole). If relaxation is considered, the mean pre-stress in coils should be of approximately 90 MPa.

5. Numerical computation

5.1. Mechanical Models

Due to the multiple contact zones taken into account in the mechanical model, calculations were realized with the COFAST3D approach [7-9] (modular developed from the CASTEM software package [10]). In this study, only the elastic behavior of magnet components is considered.

The 3D finite element models are restricted to 1/4th of the quadrupole magnet cross section, see Fig.2. The first model includes the same type of collars than those used for the LHC main quadrupole (the polar plan of coil is the same for the two layers) and have three kinds of angular wedges. The second model includes collars with polar plans different between the inner and the outer coil layers, like for the LHC main dipoles and have only two kinds of angular wedges.

Both models include two levels of collars and polar pieces, and two half coils. The front and the back collars (and the polar pieces, see in blue in Fig.2) are used to simulate the 3D-effect of the stacking in alternated layers.

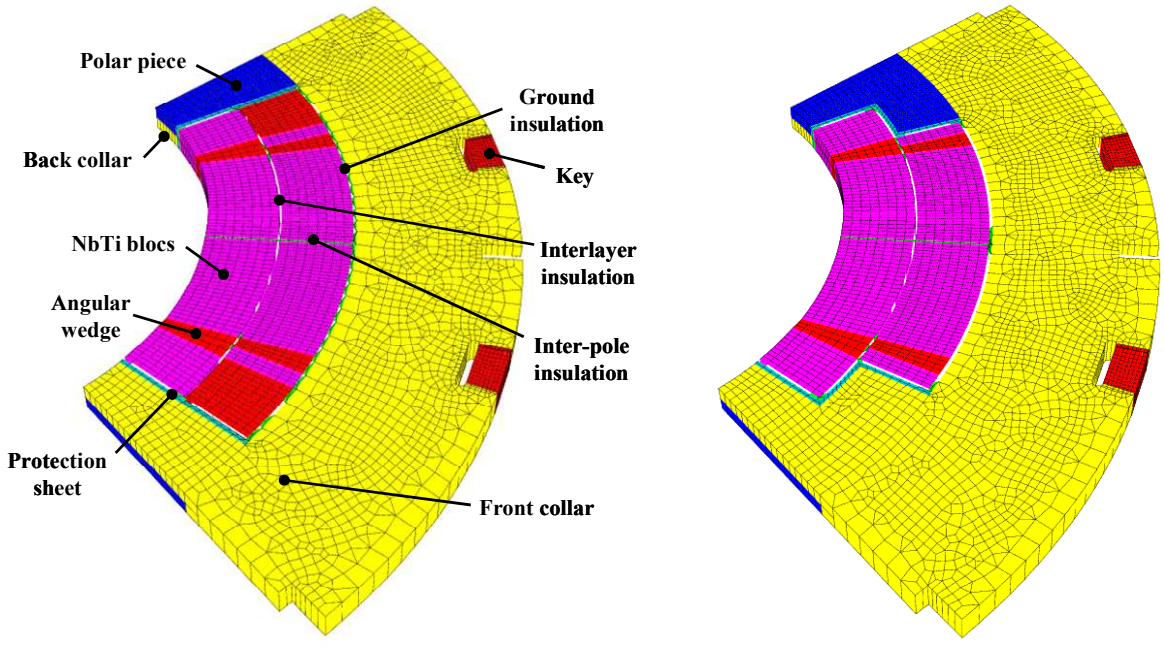

Model 1. Model 2

Fig.2: Mechanical models.

The other magnet components are:
- protection sheets (to protect the ground insulation on the polar plans),
- ground insulation,
- keys,
- interlayer insulation,
- inter-pole insulation.

Boundary conditions are imposed on the front and back collars symmetry planes and on polar pieces symmetry planes, Fig.3. Friction is considered at all contact zones (friction coefficient of 0.3). A high friction coefficient of 1.0 is taken for the contact between the coil blocs and the angular wedges.

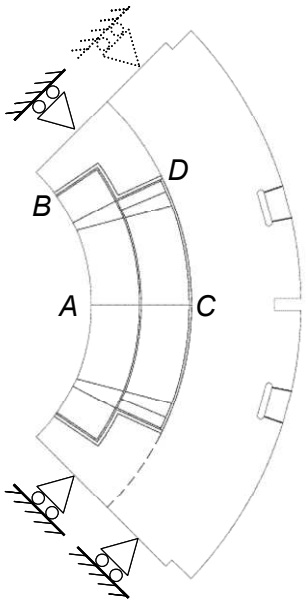

Fig.3: Boundary conditions and localization of particular points *A*, *B*, *C* and *D*.

All magnet components are assumed to be isotropic. The radial width of collars is assumed to be of 35 mm (space between coils and iron yoke). The keyways on collars have a position angle of 15 deg with the coil median plan. The keyways geometry is similar to those of the LHC main quadrupole collars.

The mechanical loading is divided into three different chronological phases corresponding to the collaring process, the cool down from 300 K to 1.8 K and the Lorentz forces application during energization:
- the collaring process is modeled by prescribing gap between the sides of the keys into collar keyways,
- the cooling is modeled by an applied thermal body force over the entire structure (by the use of integrated thermal shrinkages),
- the Lorentz forces induced at nominal current are computed using the ROXIE analysis software.

One aim of computation is to make sure that the future NbTi coils can be assembled like the LHC main quadrupole collaring process [11-14] by verifying if the following objectives are reached:

(1) all parts of coils should remain in compression at nominal current, with an acceptable stress distribution and a security margin of 10 MPa to avoid any separation on polar plan between coils and collars,

(2) during collaring, cool-down and excitation, peak stress in coils should be below 130 MPa (this value has to be confirmed by CERN) to avoid a possible degradation of the cable insulation,
(3) coil displacement should not exceed that of the actual triplets during excitation (the coil radial displacement at external radius should be below 60 μm).

Those three points directly depend on the pre-stress applied at the end of the collaring process.

5.2. Results of FEM - Comparison between model 1 and model 2

The stress level operating in coils and collars during the three loading steps (collaring, cool-down and excitation at full current) are estimated. The coil displacement during energization is given at points *A*, *B*, *C* and *D* localized in Fig.3. A relaxation of 20% of the initial stress is taken into account. Tab.2 and Tab.3 give results with mechanical model 1 and model 2, respectively. Here, we consider that the main criterion for calculation is that the minimum compressive stress on polar plan should be of 10 MPa at nominal current.

Model 1	**Collaring with keys**	**After relaxation**	**Cool down 300 K to 2 K**	**Nominal current 12720 A**
Stress σ_θ in coil blocs (MPa)				
Max	-135	-112	-91	-100
Average	-80	-66	-67	-63
Min on polar plan				**-10**
Average on polar plan				-34
Coil radial displacement Δ_r due to Lorentz forces (μm)				
Point A				84
Point B				6
Point C				**31**
Point D				-1
Max von Mises stress in collars (MPa)				
	1543	1289	1335	1651

Tab.2: Results with the mechanical model 1 assuming a minimum compressive stress on polar plan of 10 MPa at nominal current.

Model 2	**Collaring with keys**	**After relaxation**	**Cool down 300 K to 2 K**	**Nominal current 12720 A**
Stress σ_θ in coil blocs (MPa)				
Max	-152	-127	-91	-102
Average	-91	-76	-67	-64
Min on polar plan				**-10**
Average on polar plan				-27
Coil radial displacement Δ_r due to Lorentz forces (μm)				
Point A				99
Point B				39
Point C				**45**
Point D				18
Max von Mises stress in collars (MPa)				
	1918	1605	1500	1629

Tab.3: Results with the mechanical model 2 assuming a minimum compressive stress on polar plan of 10 MPa at nominal current.

Results with the mechanical model 1 seem to be better than with the mechanical model 2: in the first case, for the same criterion, lower pre-stress is needed during collaring (80 MPa versus 91 MPa) to obtain the criterion at nominal current. Peak stresses in conductor and in collars (1543 MPa versus 1918 MPa) are then lower.

Fig.4 and Fig.5 show for both models the azimuthal coil stress distribution at nominal current and the azimuthal displacement of conductor blocs due to Lorentz forces, respectively.

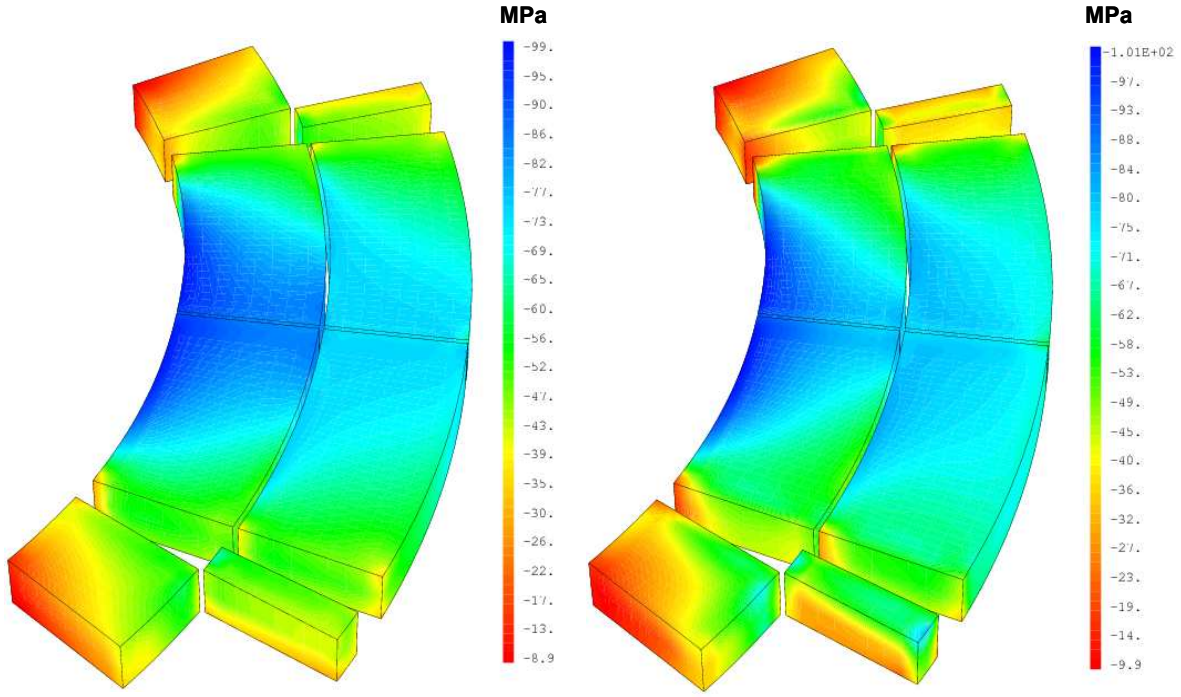

With model 1 *With model 2*

Fig.4: Azimuthal stress distribution in conductor blocs at 12720 A.

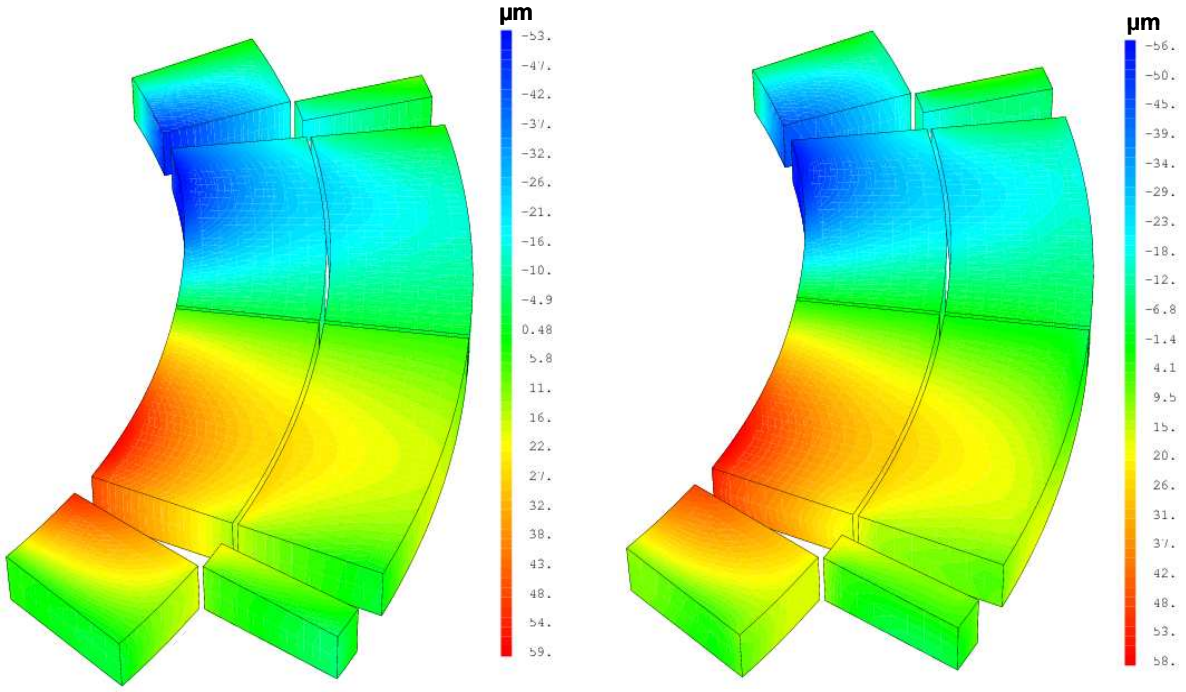

With model 1 *With model 2*

Fig.5: Azimuthal displacement of conductor blocs due to Lorentz forces.

At 12720 A, the azimuthal stress distribution in coils is quasi identical between the two models, but a “peeling stress” at the interface between conductor and angular wedge is more apparent with the model 2, especially in the inner coil layer, Fig.4. This phenomenon is principally due to thermal shrinkage differential between conductor blocs and angular wedges during cool-down.

Fig.6 shows the coil radial displacement due to Lorentz Forces during energization. The radial displacement is globally lower with the mechanical model 1, see also Tab.2 and Tab.3. Other figures allowing a comparison of both models are available in appendix of this note.

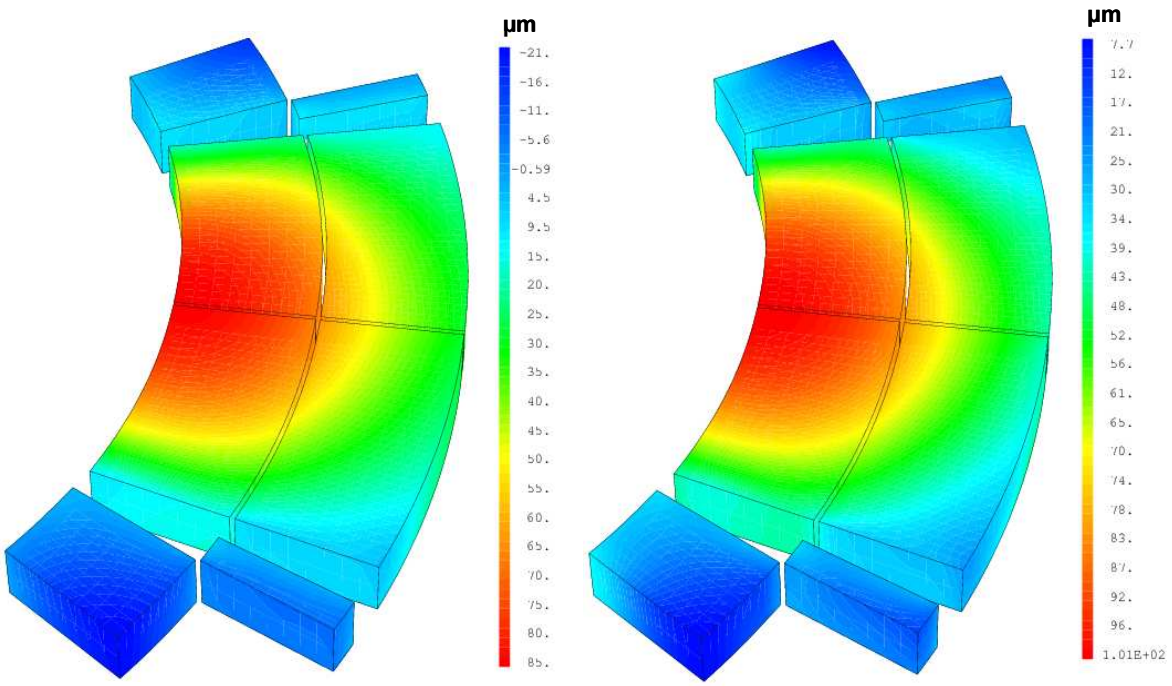

With model 1 *With model 2*

Fig.6: Radial displacement of conductor blocs due to Lorentz forces.

Von Mises stress distribution in collars after collaring is presented in Fig.7. Results show a peak stress in collars above the yield stress, see Tab.2 and Tab.3. This peak stress occurs in a highly localized region near the keyways and is of the same order than that observed in collars for the LHC main quadrupole magnets. In reality, plastic zone occurs in this region. After strain-hardening, this plastic zone remains elastic during cool-down and excitation.

Elastic-plastic calculation on collars for the LHC main quadrupole was realized by P. Vedrine in 1995-1996 [4] by assuming an elastic/perfectly plastic behavior. Results showed that the stress distribution in coils was not modified by plasticization of collars and plastic zone had no major effects on deformation of collars.

The collar material we should use for the future magnet is available at Cern: it is the Yus 130 S Nippon Steel which thermo mechanical properties are quasi-identical to the 13RM19 stainless steel used for the LHC main quadrupole, see Tab.4.

Materials *Componants*	Temp. (K)	Elastic Modulus (GPa)	Yield Strenght (MPa)	Ultimate Strength (MPa)	Integrated Thermal Expansion (mm/m)
yus 130 S Nippon Steel	300	190	445	795	
Collars	2	210	1023	1595	-2.4 to -2.6
13RM19 Stainless Steel	300	195	440	800	
Collars	2	207	1113	1634	-2.7

Tab.4: Thermo mechanical properties of Yus 130 S Nippon Steel and 13RM19 Stainless Steel.

Therefore, the peak stress in collars should not present any problem for the mechanical integrity of the structure. Nevertheless, an elastic-plastic study should be done to eliminate all doubts.

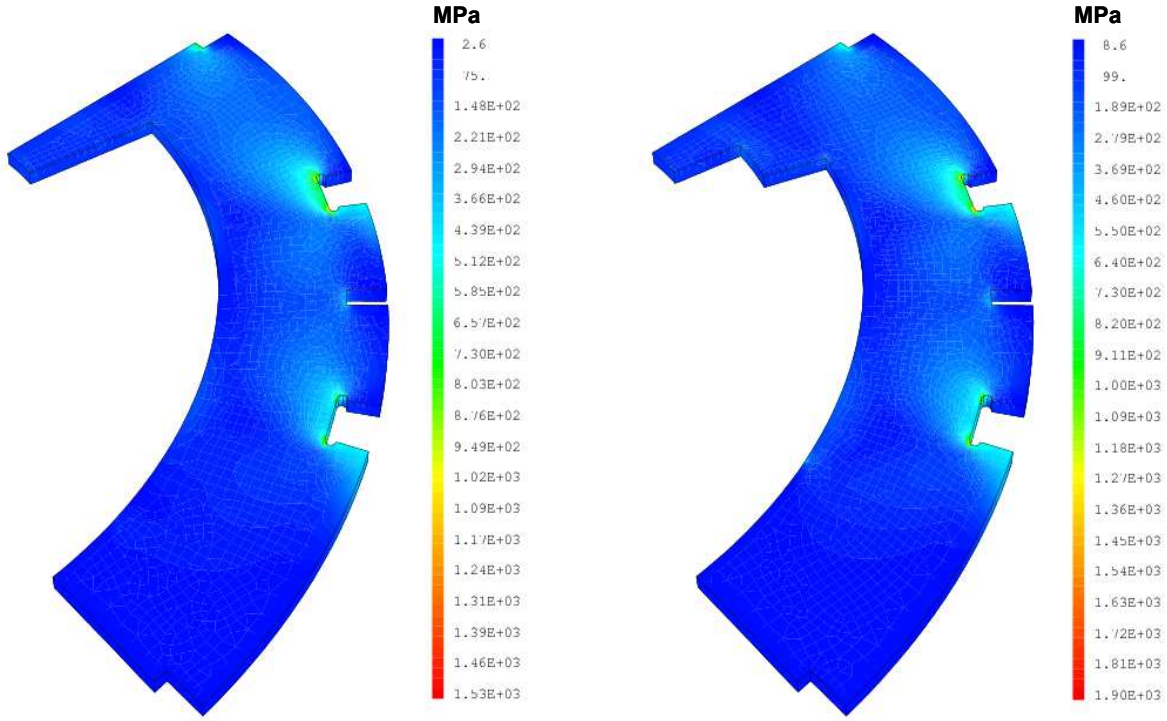

With model 1 *With model 2*

Fig.7: Von Mises stress distribution in collars after collaring (at warm).

5.3. Sensibility of the criterion on the pre-stress

Results show that we have to choose a compromise between pre-stress to impose during collaring and compressive stress to keep on polar plan at nominal current. Pre-stress should not be too high to avoid any degradation of the cable insulation and should not be too low to avoid any separation at the coil/collar interfaces at 12720 A.

The evolution of the pre-stress σ_w needed in coils after collaring (at warm) versus the minimum compressive stress $\sigma_{\min polar}$ on polar plan at nominal current is shown in Fig.8 for both models.

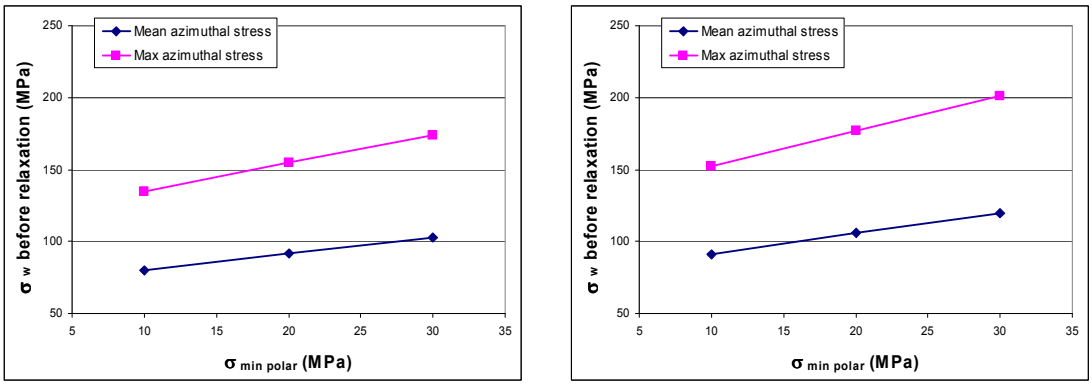

With model 1 *With model 2*

Fig.8: Evolution of pre-stress in conductor blocs versus minimum compressive stress on polar plan at 12720 A.

With model 1, an increase $\delta\sigma_{\min polar}$ = 10 MPa corresponds to a raise of $\delta\sigma_w$ = 12 MPa on the pre-stress during collaring (and of 20 MPa on the peak-stress). With model 2, an increase $\delta\sigma_{\min polar}$ = 10 MPa correspond to a raise of $\delta\sigma_w$ = 15 MPa on the pre-stress during collaring (and of 25 MPa on the peak-stress).

Tab.5 and Tab.6 give results by assuming now the following criterion for calculation: the mean compressive stress on polar plan is of 10 MPa at nominal current.

Model 1	**Collaring with keys**	**After relaxation**	**Cool down 300 K to 2 K**	**Nominal current 12720 A**
Stress σ_θ in coil blocs (MPa)				
Max	-94	-78	-56	-74
Average	-56	-46	-39	-41
Min on polar plan				-0.5
Average on polar plan				**-10**
Coil radial displacement Δ_r due to Lorentz forces (µm)				
Point A				83
Point B				12
Point C				**33**
Point D				-2
Max von Mises stress in collars (MPa)				
	1078	901	827	1085

Tab.5: Results with the mechanical model 1 assuming a mean compressive stress on polar plan of 10 MPa at nominal current.

Model 2	**Collaring with keys**	**After relaxation**	**Cool down 300 K to 2 K**	**Nominal current 12720 A**
Stress σ_θ in coil blocs (MPa)				
Max	-116	-96	-66	-79
Average	-70	-58	-42	-43
Min on polar plan				-0.3
Average on polar plan				**-10**
Coil radial displacement Δ_r due to Lorentz forces (µm)				
Point A				101
Point B				20
Point C				**45**
Point D				11
Max von Mises stress in collars (MPa)				
	1472	1231	999	1227

Tab.6: Results with the mechanical model 2 assuming a mean compressive stress on polar plan of 10 MPa at nominal current.

In this case, less pre-stress in coils is needed during the collaring process than for the previous criterion (56 MPa versus 80 MPa for model 1 and 70 MPa versus 91 MPa for model 2). The maximum stress after collaring is now below the assumed critical stress of 130 MPa (94 MPa versus 135 MPa for model 1 and 116 MPa versus 152 MPa for model 2). But here a separation of coils during excitation could operate somewhere on polar plans because $\sigma_{\min polar}$ becomes very small (less than 1 MPa for both models).

In all previous results, coil displacement at points C and D due to Lorentz forces is less than the critical displacement of 60 µm.

5.4. Loss of pre-stress during cool-down

Previous results show that the loss of pre-stress during cool-down is very low, especially with the mechanical model 1. In the following, we analyze why the loss of pre-stress is so low. The phenomenon of relaxation after collaring is not considered here.

If we consider an infinitely stiff cavity with an integrated thermal shrinkage α_f (from 300 K to 2 K), the mechanical deformation of a sample in contact with this cavity is equal to the thermal shrinkage differential $\Delta\alpha$ between the sample and the cavity during cool-down:

$$\varepsilon_w - \varepsilon_c = \alpha_s - \alpha_f = \Delta\alpha \tag{1}$$

where ε_w and ε_c are respectively the warm and the cool sample strain and α_s is the sample integrated thermal shrinkage. For analogy with coils and collars, equation (1) gives:

$$\sigma_c = \frac{E_c}{E_w}\sigma_w - E_c \times \Delta\alpha = 1.5 \times \sigma_w - (7.5 \times 5.1) \tag{2}$$

where E_c and E_w are respectively the coil Young's modulus at warm and at cool temperature and $\Delta\alpha$ is equal to the thermal shrinkage differential between coils and collars. In this case, we obtain:

$$\sigma_c = 1.5 \times \sigma_w - 38 \text{ MPa} \tag{3}$$

Numerical calculation gives the relationship between σ_c and σ_w as follow:

$$\begin{aligned} \sigma_c &= 1.4 \times \sigma_w - 25 \text{ MPa} \qquad \text{for model 1} \\ \sigma_c &= 1.4 \times \sigma_w - 38 \text{ MPa} \qquad \text{for model 2} \end{aligned} \tag{4}$$

Relationships (3) and (4) are represented in Fig.9 where the evolution of σ_c versus σ_w for the mechanical models and for the analytical approach (in red, assuming an infinitely stiff collar) is shown. The three curves are very close. It is due to the fact that for calculation the coil Young's modulus (average of 6.25 GPa) is very low compared to the collar stiffness (200 GPa). The slope difference between numerical and analytical relationships is then small.

Loss of pre-stress during cool-down is usually due to the thermal shrinkage differential $\Delta\alpha$ between coils and collars. Here, the loss of pre-stress is very low: as indicated in Eq.2, even if $\Delta\alpha$ is high, it is compensated by a very low coil Young's modulus E_c at cool temperature.

If the criterion of calculation is to obtain a minimum compressive stress on polar plan of 10 MPa at nominal current, with a pre-stress σ_w = 66 MPa at warm after relaxation, model 1 gives no loss of pre-stress during cool-down, see Tab.2. For the same criterion, model 2 gives a loss of pre-stress during cool-down of 9 MPa (from σ_w = 76 MPa to σ_c = 67 MPa), see Tab.3.

We can note that the collar shape have an effect on the azimuthal stress σ_c at cool temperature.

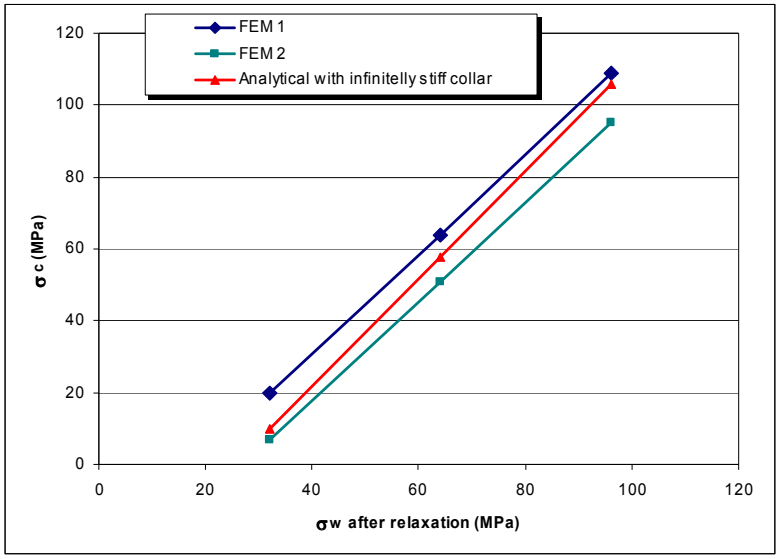

Fig.9: Evolution of the azimuthal stress in coils at cool temperature versus the azimuthal pre-stress in coils after collaring and relaxation.

5.5. Effect of the keyway angle

Fig.10. shows two configurations of keyway position angle, respectively:
- keyway angle of 15 deg with the coils median plan,
- keyway angle of 30 deg with the coils median plan.

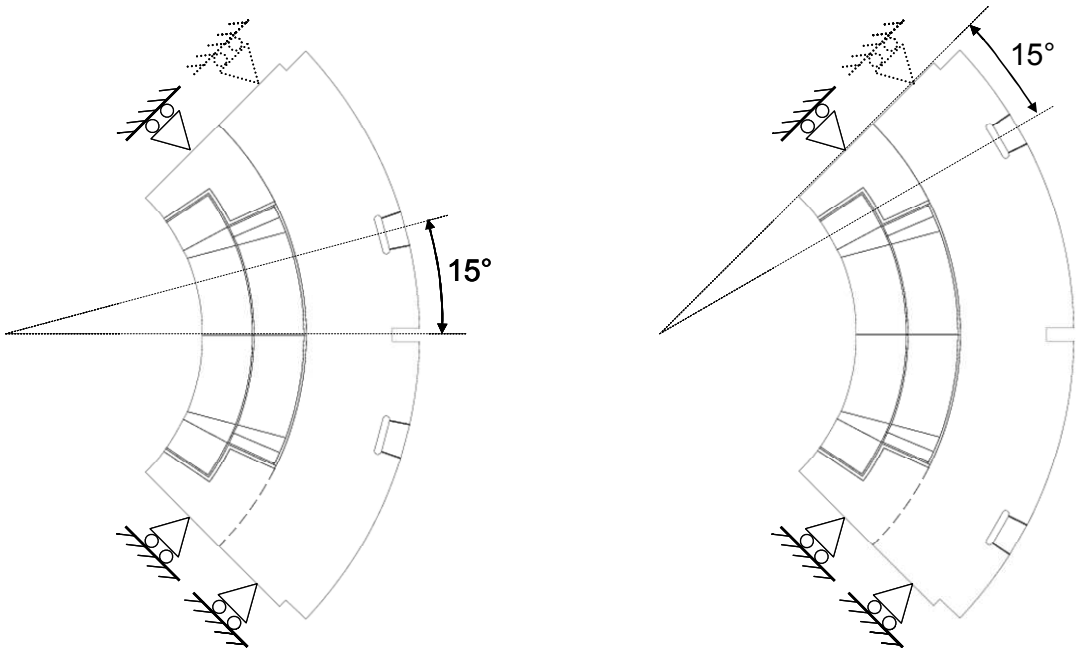

Keyway angle of 15° with the coils median plan *Keyway angle of 30° with the coils median plan*

Fig.10: Presentation of the two configuration of keyway position angle.

Tab.7 and Tab.8 give a comparison between these two configurations for both models. In this study, the reaction forces on keys are not analyzed, but the von Mises stress distribution

in keys after collaring is represented in Fig.10 and Fig.11. The criterion of calculation is to obtain a minimum compressive stress on polar plan of 10 MPa at nominal current.

Model 1	Collaring with keys		After relaxation		Cool down 300 K to 2 K		Nominal current 12720 A	
Keyway angle (deg)	**15**	**30**	**15**	**30**	**15**	**30**	**15**	**30**
Stress σ_θ in coil blocs (MPa)								
Max	-135	-119	-112	-99	-91	-81	-100	-82
Average	-80	-69	-66	-57	-67	-54	-63	-53
Min on polar plan							**-10**	**-10**
Average on polar plan							-34	-23
Coil radial displacement Δ_r due to Lorentz forces (µm)								
Point A							84	68
Point B							6	2
Point C							**31**	**18**
Point D							-1	-9
Max von Mises stress (MPa)								
in collars	1543	1354	1289	1131	1335	1137	1651	1286
in keys	429	387						

Tab.7: Comparison of results obtained with the mechanical model 1 for two keyway angle.

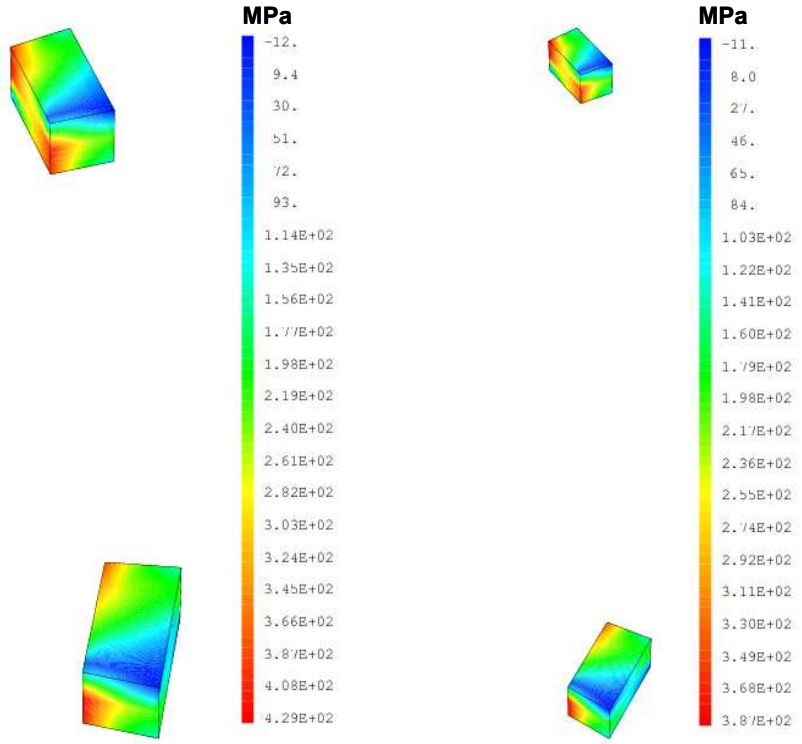

Keyway angle of 15° *Keyway angle of 30°*

Fig.11: Von Mises stress distribution in keys after collaring (at warm) obtained with model 1.

With the mechanical model 1, a keyway angle of 30 deg should give better results than a keyway angle of 15 deg: lower pre-stress is needed during collaring inducing also a lower peak stress in collars (and keys) and lower radial displacement during energization, see Tab.7 and Fig.11.

With the mechanical model 2, there is no significant difference in the results between the two configurations, see Tab.8 and Fig.12.

Model 2	Collaring with keys		After relaxation		Cool down 300 K to 2 K		Nominal current 12720 A	
Keyway angle (deg)	**15**	**30**	**15**	**30**	**15**	**30**	**15**	**30**
Stress σ_θ in coil blocs (MPa)								
Max	-152	-150	-127	-125	-91	-89	-102	-92
Average	-91	-87	-76	-72	-67	-62	-64	-60
Min on polar plan							**-10**	**-10**
Average on polar plan							-27	-23
Coil radial displacement Δ_r due to Lorentz forces (µm)								
Point A							99	94
Point B							39	39
Point C							**45**	**40**
Point D							18	16
Max von Mises stress in collars (MPa)								
in collars	1918	1896	1605	1585	1500	1509	1629	1555
in keys	568	600						

Tab.8: Comparison of results obtained with the mechanical model 2 for two keyway angle.

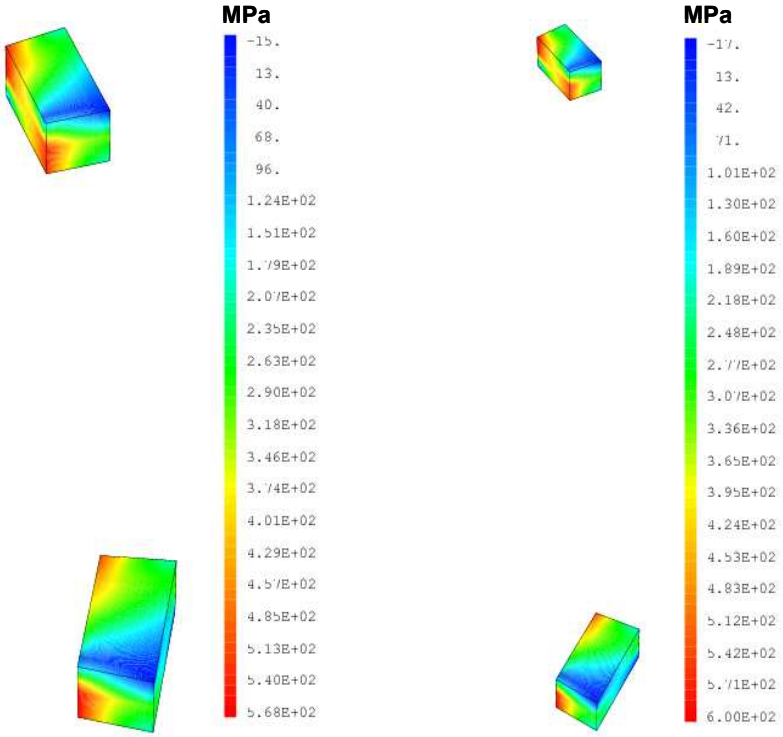

Keyway angle of 15° *Keyway angle of 30°*

Fig.12: Von Mises stress distribution in keys after collaring (at warm) obtained with model 2.

6. Conclusion

Mechanical computation gives an estimation of stress in coils and in collars at each main phase which are collaring, cool-down and excitation. Coil displacement due to Lorentz forces is also analyzed.

The first model includes the same kind of collars than those used for the LHC main quadrupole magnets. The second model includes collars with polar plans different between the inner and the outer coil layers.

The first model seems to give better results than the second one for the following reasons:

- lower azimuthal pre-stress is needed in coils after collaring for the same criterion of calculation (because there is quasi-no loss of pre-stress during cool-down).
- lower peak stress in collars,
- lower "peeling stress" at the interface conductor blocs/angular wedges after cool-down,
- lower radial displacement during energization (from 0 A to 12720 A).

A keyway angle of 30 deg (instead of 15 deg) gives little better results with the model 1, but no significant difference in results obtained with the model 2. Note that the reaction forces on keys are not analyzed.

For the future NbTi coils, a collaring process like that used for the LHC main quadrupole magnets should be possible to apply. Nevertheless, in all cases, it will be necessary to choose a compromise on the imposed pre-stress after collaring: pre-stress should not be too high to avoid a damage of the cable insulation and should not be too low to avoid separation between coils and collars on polar plans at nominal current.

But there are some points that are needed to be analyzed to determine the real pre-stress:

- What is the maximum azimuthal stress we can put in coil before having a damage of the cable insulation?
- What is the real thermo mechanical behavior of conductor blocs? Values of Young's modulus at cool temperature and of thermal shrinkage for conductor stacks should be experimentally determined (CERN).
- What is the real relaxation level after collaring? It should also be experimentally determined (CERN).

An elastic-plastic study should be done to verify the effect of local collar plasticization (around the keyway) on the stress distribution in coils and on the coil displacement, but, taken into account of LHC main quadrupole knowledge, this can be performed later.

7. References

[1] ROXIE, *trademark from CERN*, Switzerland.

[2] P. Ferracin, "Mechanical and magnetic analysis of the large hadron collider main dipole", *Tesi di dottorato*, march 2002.

[3] P. Védrine, B. Gallet, C. Nouvel, "Measurement of Thermo-Mechanical Properties of NbTi Windings for Accelerator Magnets", *IEEE Trans. Appl. Supercond.*, Vol. 9 No. 2, pp. 1705-1708, June 1999.

[4] P. Védrine, "Pré-étude mécanique du nouveau quadripôles LHC", *Internal report 5C2390T-00920 001 96, CEA/Saclay* – STCM, 1996.

[5] F. Markley *et al.*, "Investigation of the Mechanical Properties of Superconducting Coils", *Supercollider 3, Plenum Press*, 1991.

[6] F. Markley *et al.*, "Stress Relaxation in SSC Collared Coils and their components materials", *Supercollider 4, Plenum Press*, 1991.

[7] L. Champaney, "Une nouvelle approche modulaire pour l'analyse d'assemblage de structures tri-dimensionnelles", *Thèse de l'ENS de Cachan*, juin 1996.

[8] L. Champaney, “Etude de l'influence de phénomènes de frottement dans le calcul mécanique en élasticité linéaire par éléments finis d'une section de quadripôle LHC”, *LMT-Cachan*, France, 1998.
[9] C. Gourdin, L. Champaney, P. Vedrine, “The Use of a New Modular Approach in the Mechanical Design of Superconducting Magnets”, *Magnet Technology 17*, Geneva, Swiss, Sept. 2001.
[10] CASTEM 2000, *trademark from CEA/Saclay*, France.
[11] M. Chapman, “Analyse mécanique des quadripôles LHC #9”, *Internal report 102 02A 000 TC 38, CEA/Saclay* – STCM, 1990.
[12] L. Grillet, “Calcul mécanique des quadripôles du LHC”, *Rapport de Stage de Maîtrise ENS-Cachan*, Option Génie Mécanique, Sept. 1995.
[13] C. Forest Divonne, “Calcul mécanique des quadripôles du LHC”, *Rapport de Stage de Maîtrise ENS6 Cachan*, Option Génie Mécanique, Sept. 1996.
[14] M. Peyrot *et al.*, “Construction of the new prototype of main quadrupole cold mass for the arc short straight sections of LHC”, *IEEE Trans. Appl. Supercond.*, Vol. 10 No. 1, pp. 170-173, 2000.

8. Appendix

This appendix gives a complement of results obtained at paragraph 5.1. Here the complete two half coils (with angular wedges) and the ground insulation are represented.

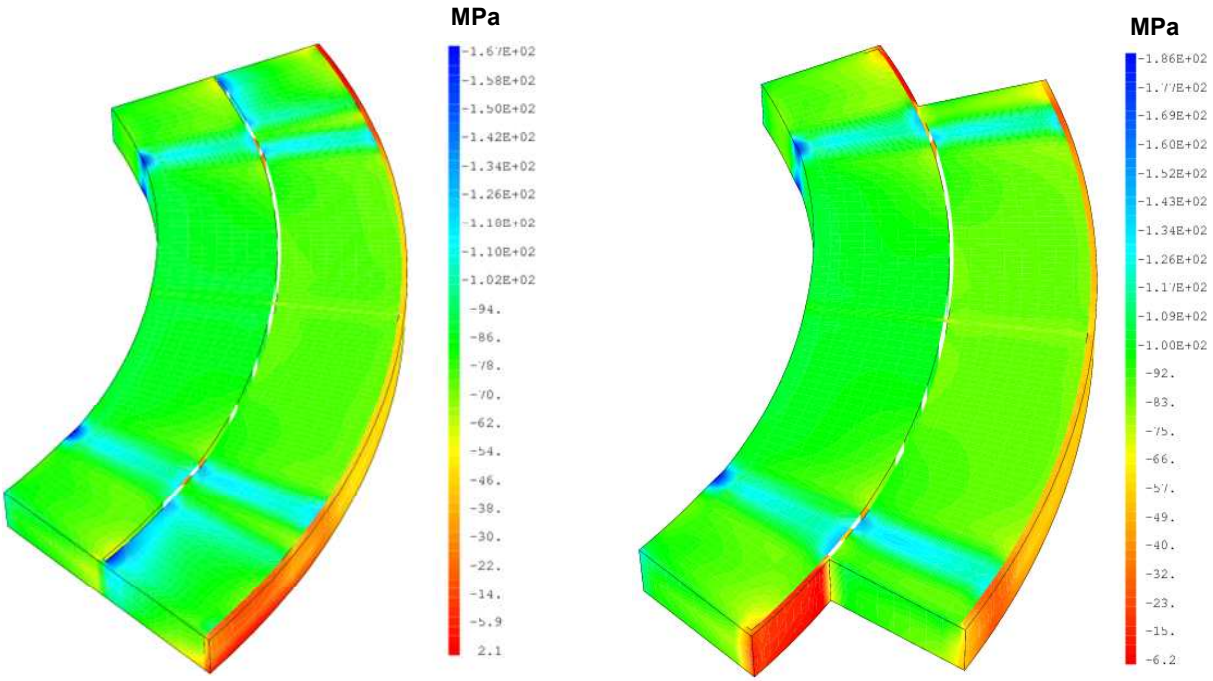

With model 1 *With model 2*

Fig.A1: Azimuthal stress distribution in coils after collaring (before relaxation).

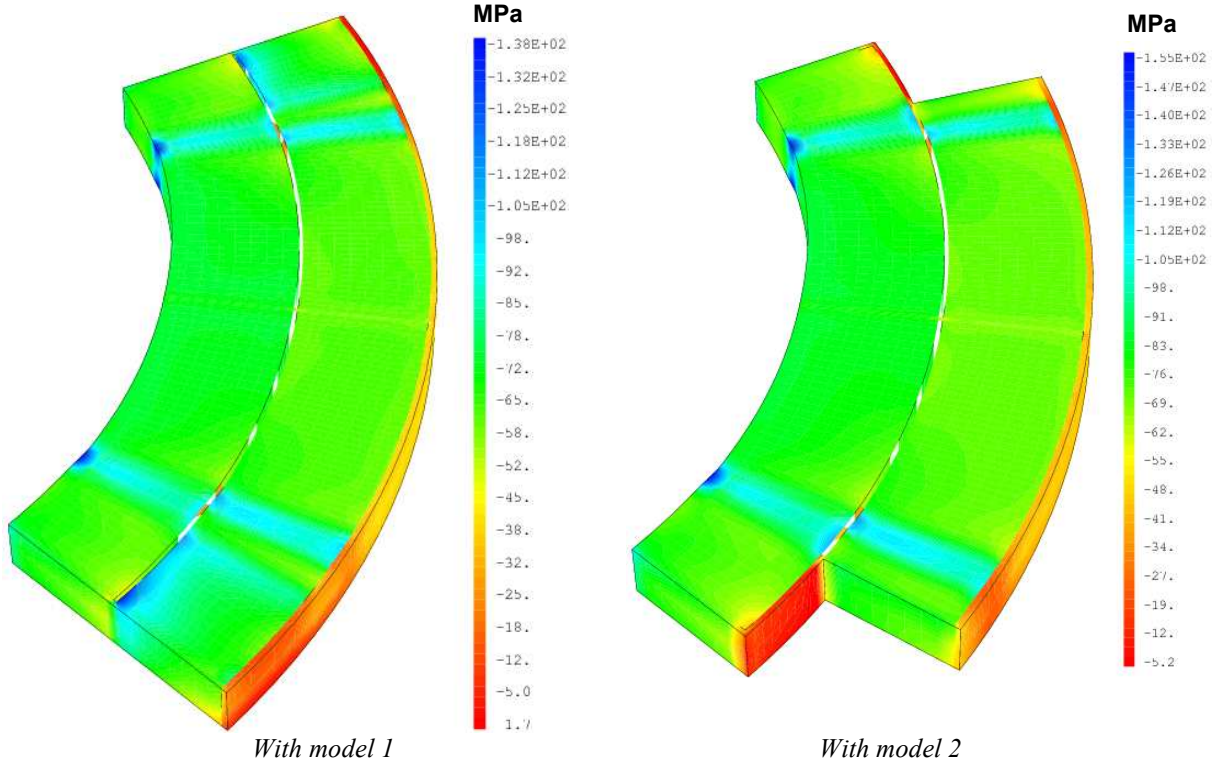

With model 1 *With model 2*

Fig.A2: Azimuthal stress distribution in coils after collaring (after relaxation).

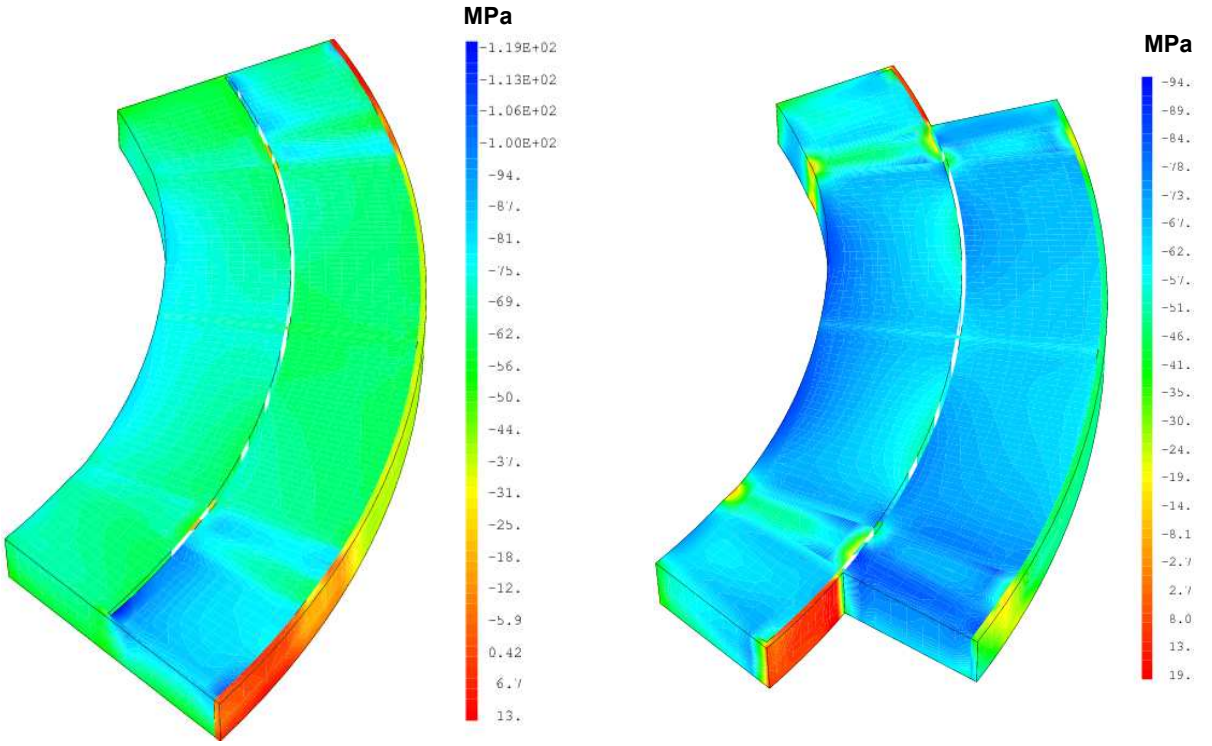

With model 1 *With model 2*

Fig.A3: Azimuthal stress distribution in coils at cool temperature.

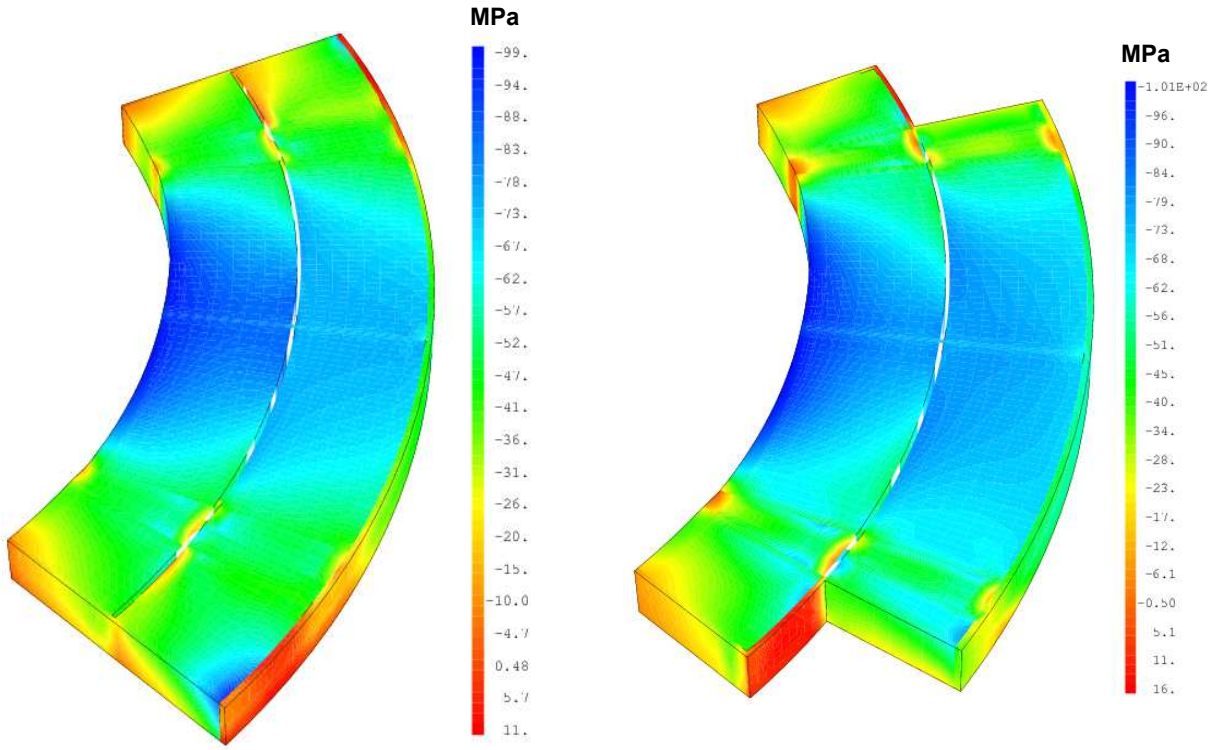

With model 1 *With model 2*

Fig.A4: Azimuthal stress distribution in coils at 12720 A.

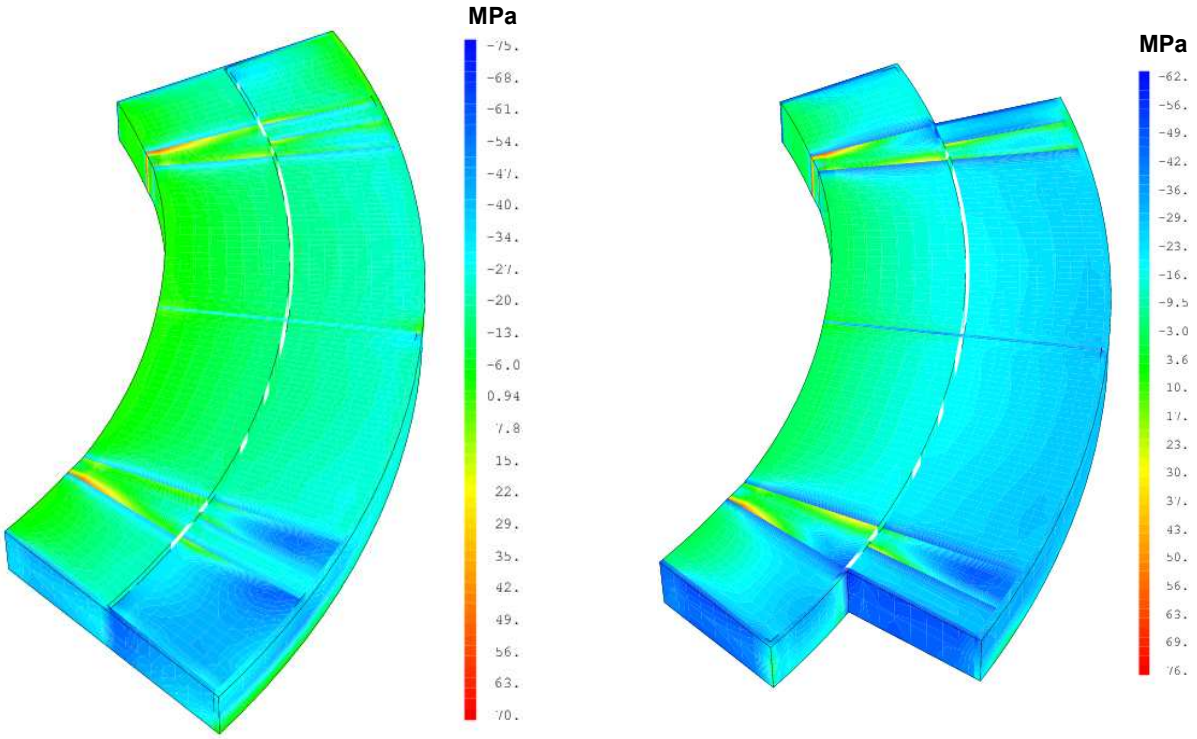

With model 1 *With model 2*

Fig.A5: Radial stress distribution in coils after collaring (before relaxation).

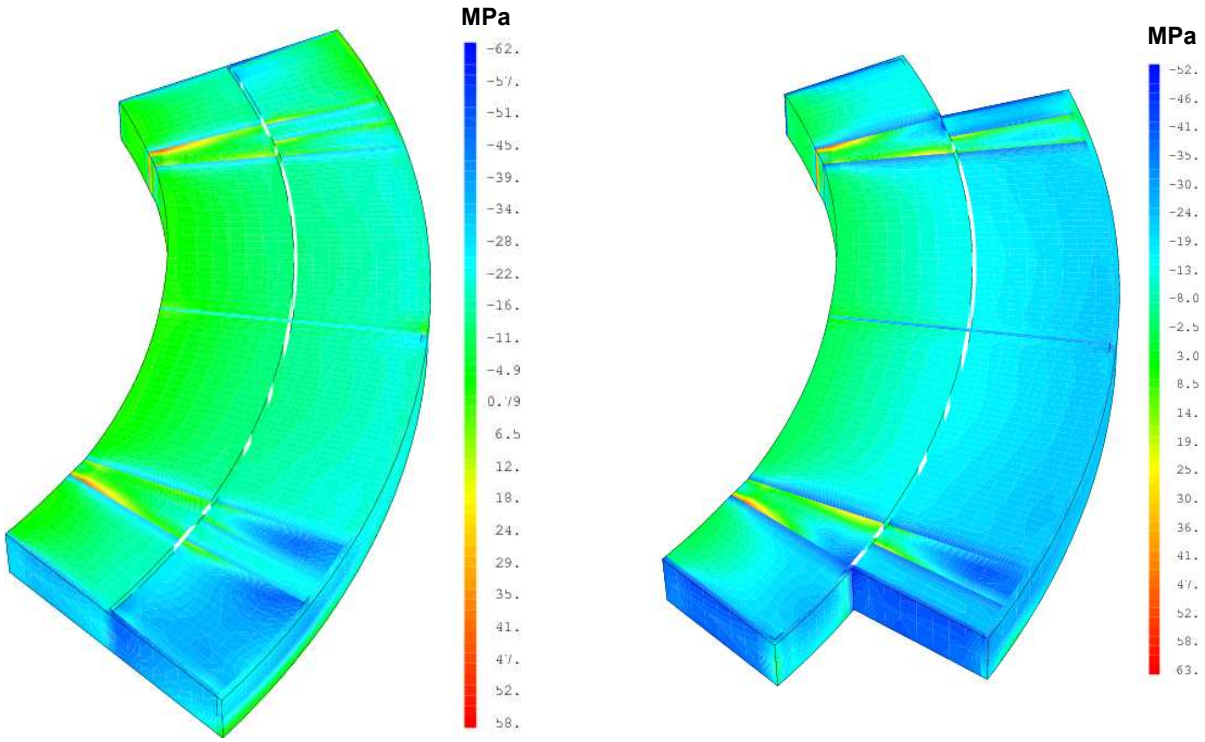

With model 1 *With model 2*

Fig.A6: Radial stress distribution in coils after collaring (after relaxation).

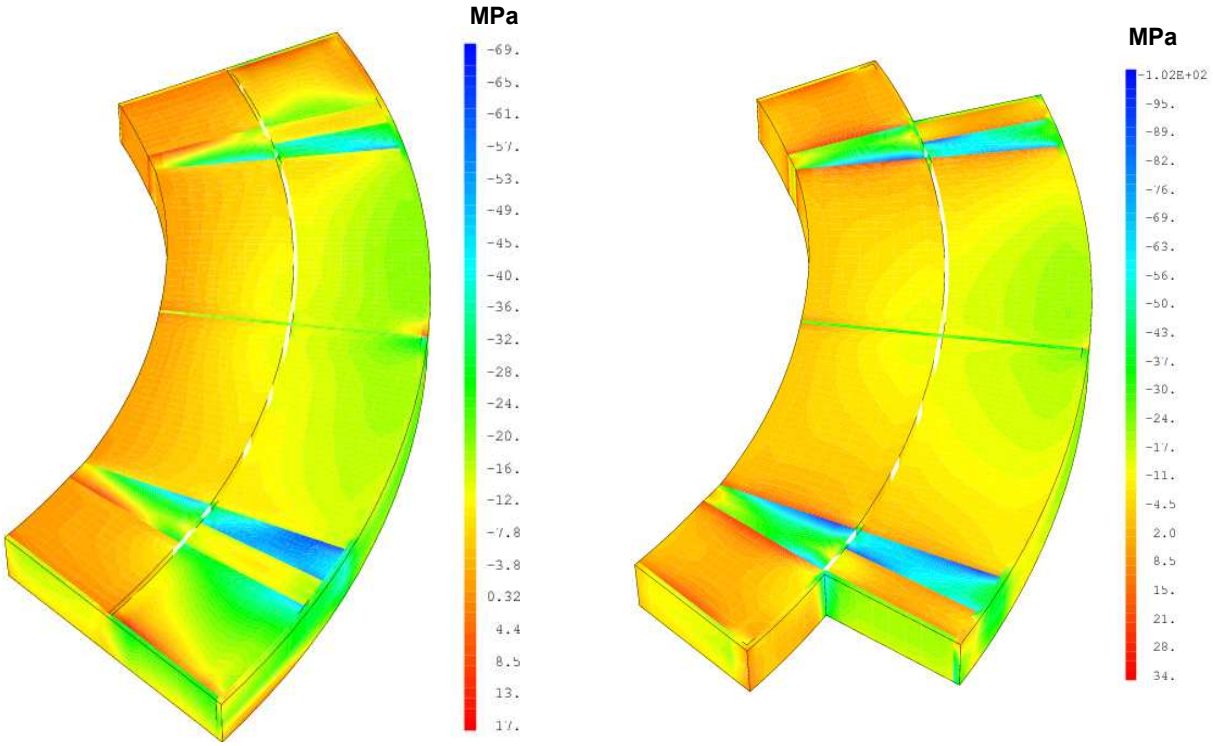

With model 1 *With model 2*

Fig.A7: Radial stress distribution in coils at cool temperature.

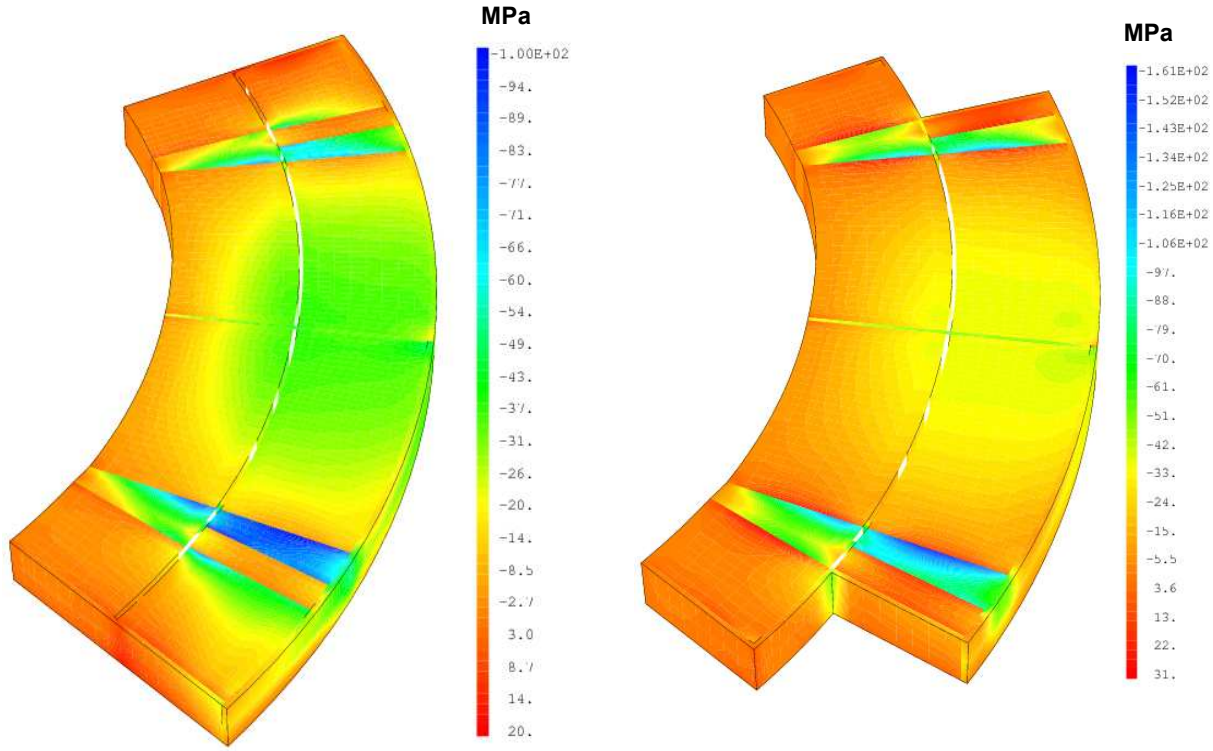

With model 1 *With model 2*

Fig.A8: Radial stress distribution in coils at 12720 A.

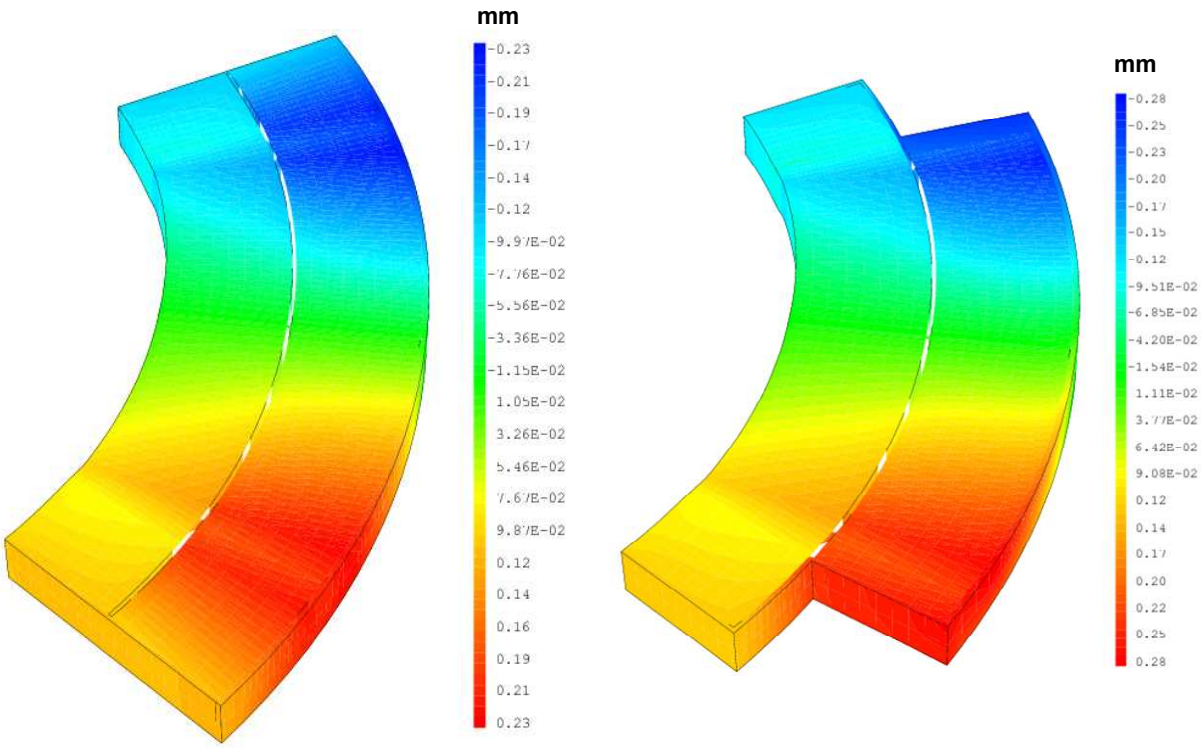

With model 1 *With model 2*

Fig.A9: Azimuthal displacement in coils after collaring.

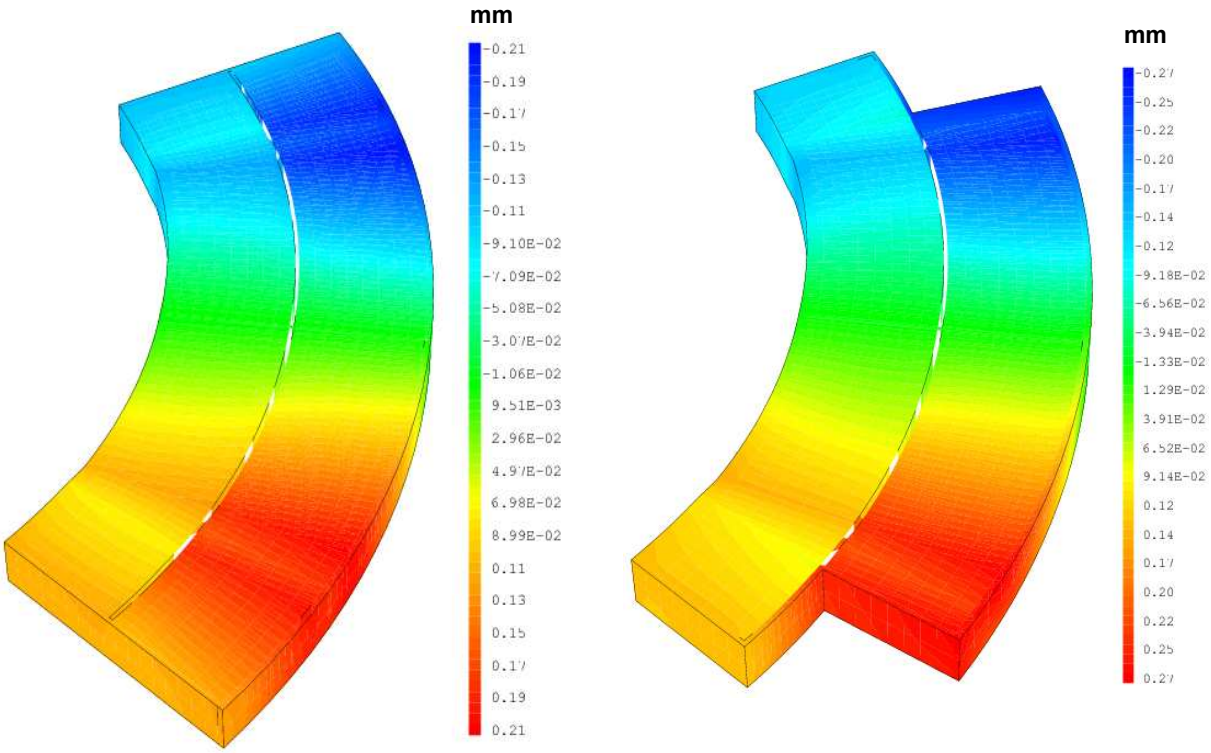

With model 1 *With model 2*

Fig.A10: Azimuthal displacement in coils at cool temperature.

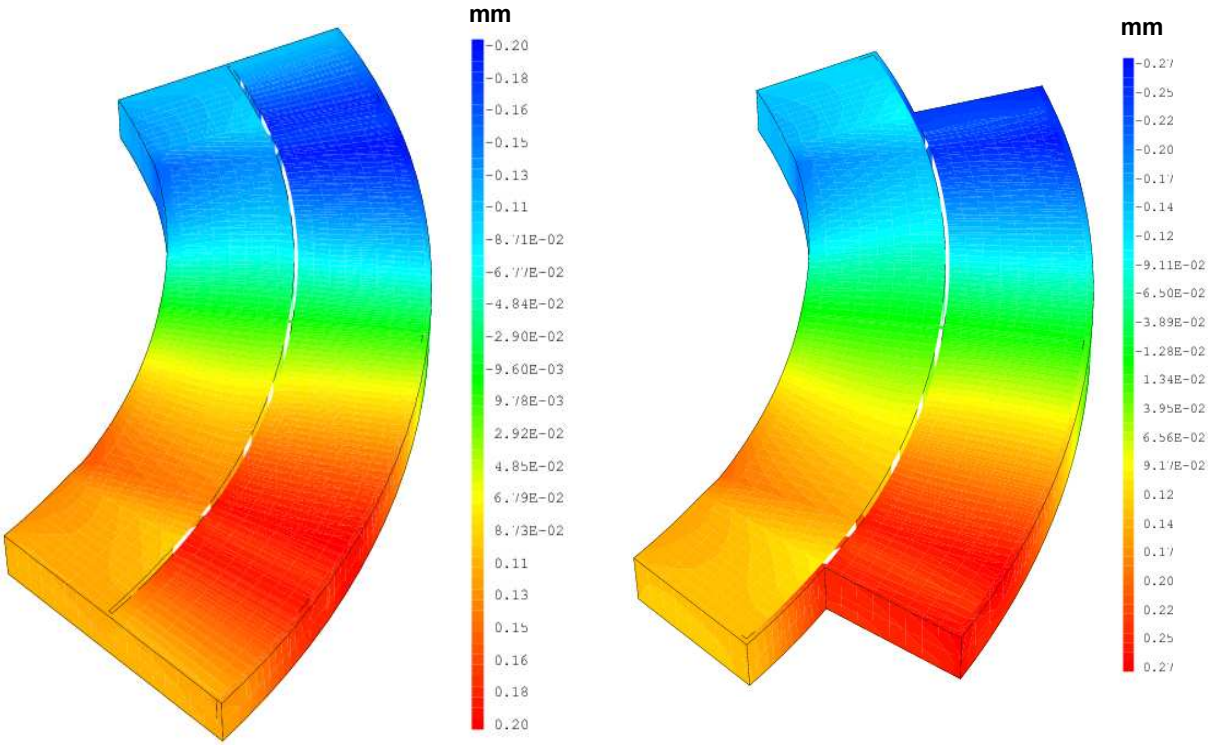

With model 1 *With model 2*

Fig.A11: Azimuthal displacement in coils at 12720 A.

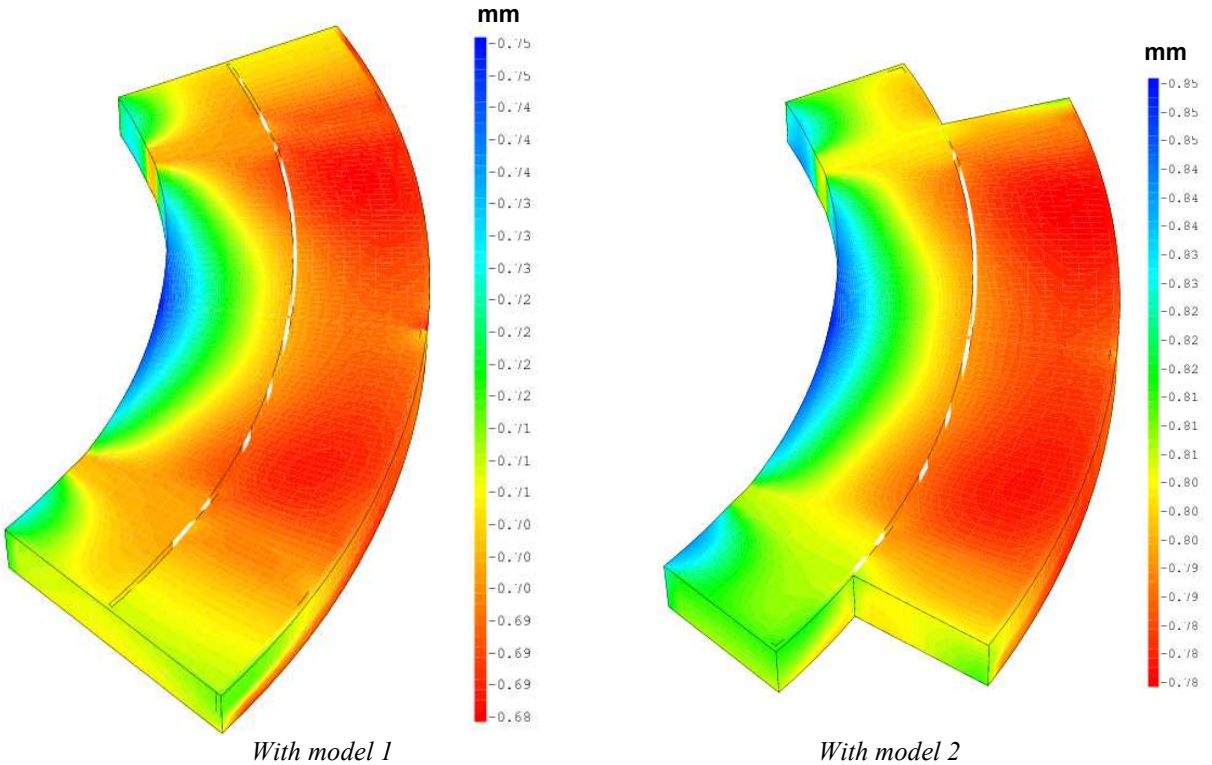

With model 1 *With model 2*

Fig.A12: Radial displacement in coils after collaring.

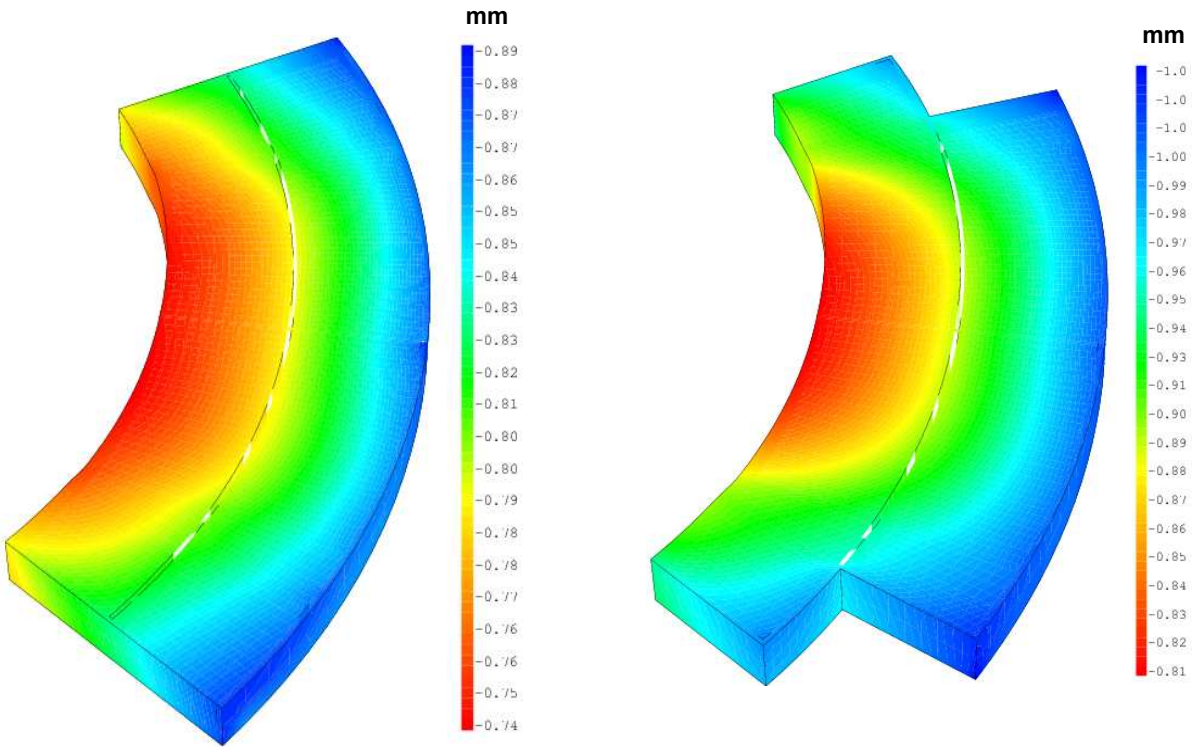

With model 1 *With model 2*

Fig.A13: Radial displacement in coils at cool temperature.

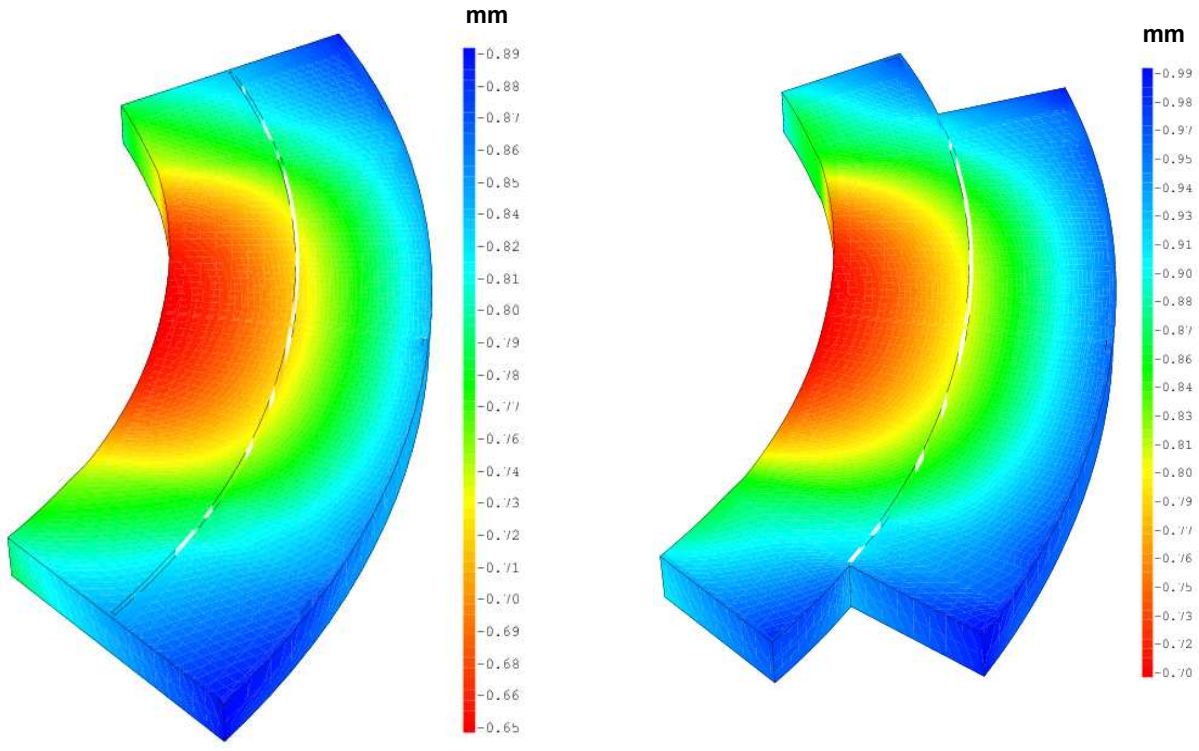

With model 1 *With model 2*

Fig.A14: Radial displacement in coils at 12720 A.